Metabasin Approach for Computing the Master Equation Dynamics of Systems with Broken Ergodicity

John C. Mauro,*,† Roger J. Loucks,†,‡ and Prabhat K. Gupta§

Science & Technology Division, Corning Incorporated, Corning, New York 14831, Department of Physics & Astronomy, Alfred University, Alfred, New York 14802, and Department of Materials Science and Engineering, The Ohio State University, Columbus, Ohio 43210

Received: April 23, 2007; In Final Form: May 31, 2007

We propose a technique for computing the master equation dynamics of systems with broken ergodicity. The technique involves a partitioning of the system into components, or metabasins, where the relaxation times within a metabasin are short compared to an observation time scale. In this manner, equilibrium statistical mechanics is assumed within each metabasin, and the intermetabasin dynamics are computed using a reduced set of master equations. The number of metabasins depends upon both the temperature of the system and its derivative with respect to time. With this technique, the integration time step of the master equations is governed by the observation time scale rather than the fastest transition time between basins. We illustrate the technique using a simple model landscape with seven basins and show validation against direct Euler integration. Finally, we demonstrate the use of the technique for a realistic glass-forming system (viz., selenium) where direct Euler integration is not computationally feasible.

1. Introduction

The master equation approach is a useful technique for modeling the dynamics of nonequilibrium statistical mechanical systems.[1−5] The approach involves constructing a set of coupled rate equations, with one equation for each available microstate in the system. For a system with Ω microstates, labeled $i, j \in \{1, 2, ..., \Omega\}$, the set of master equations is given by eq 1;

$$\frac{dp_i}{dt} = \sum_{j \neq i} (K_{ji}p_j - K_{ij}p_i) \tag{1}$$

where p_i denotes the probability of occupying state i, K_{ji} is the transition rate from state j to state i, and K_{ij} is the rate of reverse transition. The occupation probabilities are subject to the constraint given by eq 2 for all times t.

$$\sum_i p_i(t) = 1 \tag{2}$$

Assuming detailed balance, the master equation dynamics of eq 1 always follow the relaxation of a system toward an equilibrium state (e.g., during isothermal relaxation).

A recent application of the master equation approach by Mauro and Varshneya[6,7] considers the problem of glass transition in an energy landscape. Rather than starting in a nonequilibrium state and following the dynamics of a system as it relaxes toward equilibrium, Mauro and Varshneya consider a liquid system initially at equilibrium. Departure into the nonequilibrium glassy regime is computed by solving a set of master equations where the transition rates are functions of an arbitrary cooling path, $K_{ij}[T(t)]$. As the system is cooled through the glass transition range, the relaxation time becomes longer than the observation time scale (related to the inverse of the cooling rate). The glass transition is, in effect, a transition from an ergodic supercooled liquid state to a nonergodic glassy state.[8−16] At low temperatures the occupation probabilities p_i are effectively frozen as the system becomes trapped in local regions of the energy landscape.

In practice, the transition rates K_{ij} can span over several orders of magnitude. Because the integration time step for solving the system of master equations is limited by the inverse of the fastest rate, direct integration of eq 1 is often inefficient. Moreover, an analytical solution for the system of the master equations, in general, assumes constant rate parameters; in the approach of Mauro and Varshneya, the rate parameters change with time as the initially liquid system cools to a glassy state.

In this paper, we propose an efficient algorithm for computing the master equation dynamics of broken ergodic systems with highly disparate rate parameters. Our method is based on a partitioning of the phase space into components or metabasins, which are chosen to satisfy the following two criteria: (1) The relaxation time scale within a metabasin is short compared to the inverse of the cooling rate (i.e., the observation time scale over which the temperature can be assumed constant). Hence, the probability distribution within a metabasin follows equilibrium statistical mechanics within the restricted ensemble. (2) The intermetabasin relaxation time scale is too long to allow for equilibration on the observation time scale. Consequently, the intermetabasin dynamics are computed based on a reduced set of master equations, with one master equation for each metabasin.

The first criterion corresponds to Palmer's condition of internal ergodicity for broken ergodic systems.[17] The second criterion is a generalization of Palmer's condition of confinement; whereas Palmer's work forbids transitions between metabasins, in our work, these transitions are allowed and are computed using a reduced set of master equations. The intermetabasin transition rates are calculated at each temperature step based on the individual transition rates between microstates.

* To whom correspondence should be sent. E-mail: mauroj@corning.com.
† Corning Incorporated.
‡ Alfred University.
§ The Ohio State University.

10.1021/jp0731194 CCC: $37.00
Published on Web 07/25/2007

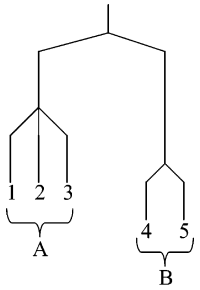

Figure 1. Simple system with two groups of degenerate microstates.

In this manner, our approach can account for a continuous breakdown of ergodicity as the system cools through the glass transition range.

Note that, by decoupling the inter- and intrametabasin dynamics, we are able to solve a reduced set of master equations on the natural time scale of the experiment (i.e., the observation time scale defined by the cooling rate). In other words, the integration time step is governed by the cooling rate rather than by the fastest microscopic transition rate. As we demonstrate later in this paper, this decoupling technique is especially useful for computing the dynamics of realistic glass-forming systems.

Our paper is organized as follows. Section 2 shows how the number of master equations can be reduced by accounting for the degeneracy of the microstates. In Section 3 we derive the equations for intra- and intermetabasin dynamics. The actual partitioning of the system into metabasins is accomplished using the algorithm in Section 4. Section 5 describes an approximation that can be used in the case of unbalanced intermetabasin transition rates. Section 6 describes the steps for combining the intra- and intermetabasin dynamics into one algorithm. In Section 7 we show the validation of our technique against direct Euler integration for a simple seven-basin system. Finally, Section 8 demonstrates the application of the metabasin technique to a realistic glass-forming system (viz., selenium).

2. Master Equations and Degeneracy

Our first task is to reduce the number of master equations by accounting for degenerate states. To elucidate how degeneracy can be incorporated into the system of master equations, let us consider the simple example of Figure 1, where there are five distinct microstates labeled 1−5. The complete system of master equations for the five states is as follows.

$$\frac{dp_1}{dt} = K_{21}p_2 + K_{31}p_3 + K_{41}p_4 + K_{51}p_5 - (K_{12} + K_{13} + K_{14} + K_{15})p_1 \quad (3)$$

$$\frac{dp_2}{dt} = K_{12}p_1 + K_{32}p_3 + K_{42}p_4 + K_{52}p_5 - (K_{21} + K_{23} + K_{24} + K_{25})p_2 \quad (4)$$

$$\frac{dp_3}{dt} = K_{13}p_1 + K_{23}p_2 + K_{43}p_4 + K_{53}p_5 - (K_{31} + K_{32} + K_{34} + K_{35})p_3 \quad (5)$$

$$\frac{dp_4}{dt} = K_{14}p_1 + K_{24}p_2 + K_{34}p_3 + K_{54}p_5 - (K_{41} + K_{42} + K_{43} + K_{45})p_4 \quad (6)$$

$$\frac{dp_5}{dt} = K_{15}p_1 + K_{25}p_2 + K_{35}p_3 + K_{45}p_4 - (K_{51} + K_{52} + K_{53} + K_{54})p_5 \quad (7)$$

We can reduce the number of master equations from five to two by accounting for the degeneracy of the system (microstates 1−3 are degenerate, as are microstates 4 and 5). We define the two unique states as A and B, with degeneracies given by $g_A = 3$ and $g_B = 2$, respectively. Likewise, there are only four unique rate parameters.

$$K_{12} = K_{21} = K_{13} = K_{31} = K_{23} = K_{32} \quad (8)$$

$$K_{14} = K_{24} = K_{34} = K_{15} = K_{25} = K_{35} \quad (9)$$

$$K_{41} = K_{42} = K_{43} = K_{51} = K_{52} = K_{53} \quad (10)$$

$$K_{45} = K_{54} \quad (11)$$

Assuming the system starts in equilibrium, we have the following relationships;[4]

$$p_1(t) = p_2(t) = p_3(t) \quad (12)$$

and

$$p_4(t) = p_5(t) \quad (13)$$

The probabilities of occupying states A and B are shown in eqs 14 and 15, respectively.

$$P_A = p_1 + p_2 + p_3 = g_A p_1 \quad (14)$$

$$P_B = p_4 + p_5 = g_B p_4 \quad (15)$$

The rates of change of P_A and P_B are given in eqs 16 and 17, respectively.

$$\frac{dP_A}{dt} = \frac{dp_1}{dt} + \frac{dp_2}{dt} + \frac{dp_3}{dt} \quad (16)$$

$$\frac{dP_B}{dt} = \frac{dp_4}{dt} + \frac{dp_5}{dt} \quad (17)$$

Substituting in the original master eqs 3−7, we obtain eqs 18 and 19.

$$\frac{dP_A}{dt} = (g_A - 1)K_{21}(p_1 + p_2 + p_3) + g_A K_{41}(p_4 + p_5) - (g_A - 1)K_{12}(p_1 + p_2 + p_3) - g_B K_{14}(p_1 + p_2 + p_3) \quad (18)$$

$$\frac{dP_B}{dt} = g_B K_{14}(p_1 + p_2 + p_3) + (g_B - 1)K_{54}(p_4 + p_5) - g_A K_{41}(p_4 + p_5) - (g_B - 1)K_{45}(p_4 + p_5) \quad (19)$$

These equations reduce to eqs 20 and 21, respectively.

$$\frac{dP_A}{dt} = g_A K_{41} P_B - g_B K_{14} P_A \quad (20)$$

$$\frac{dP_B}{dt} = g_B K_{14} P_A - g_A K_{41} P_B \quad (21)$$

By defining $\tilde{K}_{AB} = g_B K_{14}$ as the effective transition rate from state A to state B and $\tilde{K}_{BA} = g_A K_{41}$ as the rate of the reverse transition, the new system of master equations can be written in the familiar forms shown in eqs 22 and 23.

$$\frac{dP_A}{dt} = \tilde{K}_{BA}P_B - \tilde{K}_{AB}P_A \quad (22)$$

$$\frac{dP_B}{dt} = \tilde{K}_{AB}P_A - \tilde{K}_{BA}P_B \quad (23)$$

Generalizing to an arbitrary system, the probability of occupying any unique state A is equal to eq 24.

$$P_A = \sum_{i\in A} p_i = g_A p_{i\in A} \quad (24)$$

where $p_{i\in A}$ is the probability of occupying any of the individual microstates i in A. The generalized set of master equations is given by eq 25;

$$\frac{dP_A}{dt} = \sum_{B\neq A} (\tilde{K}_{BA}P_B - \tilde{K}_{AB}P_A) \quad (25)$$

where

$$\tilde{K}_{AB} = g_B K_{i\in A, j\in B} \quad (26)$$

3. Master Equations Dynamics with the Metabasin Approach

The next step is to rewrite the master equations in terms of a reduced set of metabasins,[18−22] where each metabasin contains a group of microstates that are mutually accessible at a given temperature and for a given observation time. Hence, we assume equilibrium statistical mechanics within a metabasin. The metabasins themselves are separated from each other by larger activation barriers such that intermetabasin transitions occur on a time scale slower than the observation time. The intermetabasin dynamics are computed using a reduced set of master equations.

Our algorithm for partitioning of the system into metabasins is presented in Section 4. In this section, we derive the equations for intra- and intermetabasin dynamics.

3.1. Equilibrium Statistical Mechanics Within a Metabasin. Let us define f_α as the probability of occupying a given metabasin α;

$$f_\alpha = \sum_{A\in\alpha} P_A = \sum_{A\in\alpha}\sum_{i\in A} p_i \quad (27)$$

where the summation is restricted to those states within metabasin α. Because every microstate is a member of one and only one metabasin, the metabasin probabilities satisfy eq 28:

$$\sum_\alpha f_\alpha = \sum_\alpha \sum_{A\in\alpha}\sum_{i\in A} p_i = 1 \quad (28)$$

Because the metabasins are chosen to satisfy the condition of internal ergodicity, we can compute the probability distribution of microstates within a metabasin using equilibrium statistical mechanics over a restricted ensemble. The partition function restricted to any metabasin α is defined by eq 29;

$$Q_\alpha = \sum_{A\in\alpha} g_A \exp\left(-\frac{U_{i\in A}}{kT}\right) \quad (29)$$

where T is the absolute temperature of the system, which can vary with time. With this definition, the probability of occupying any microstate i in metabasin α is given by eq 30.

$$p_{i\in\alpha} = \frac{f_\alpha}{Q_\alpha}\exp\left(-\frac{U_i}{kT}\right) \quad (30)$$

By accounting for degeneracy, we get eq 31.

$$P_A = g_A p_{i\in A} = \frac{f_\alpha}{Q_\alpha} g_A \exp\left(-\frac{U_{i\in A}}{kT}\right) \quad (31)$$

This can be rewritten as eq 32;

$$P_A = \frac{f_\alpha}{Q_\alpha}\exp\left(-\frac{F_A}{kT}\right) \quad (32)$$

where F_A is the free energy of state A, defined as eq 33;

$$F_A = U_{i\in A} - TS_A \quad (33)$$

where S_A is the Boltzmann entropy.

$$S_A = k \ln g_A \quad (34)$$

3.2. Intermetabasin Dynamics. The intermetabasin dynamics can be computed using a reduced set of master equations, with one equation for each metabasin. Let us consider the simple two-metabasin system in Figure 2. The first metabasin (labeled α) contains two unique states (A and B); the second metabasin (labeled β) contains three unique states (C, D, and E). The dynamics of the system is given by the following equations;

$$\frac{dP_A}{dt} = \tilde{K}_{BA}P_B + \tilde{K}_{CA}P_C + \tilde{K}_{DA}P_D + \tilde{K}_{EA}P_E - (\tilde{K}_{AB} + \tilde{K}_{AC} + \tilde{K}_{AD} + \tilde{K}_{AE})P_A \quad (35)$$

$$\frac{dP_B}{dt} = \tilde{K}_{AB}P_A + \tilde{K}_{CB}P_C + \tilde{K}_{DB}P_D + \tilde{K}_{EB}P_E - (\tilde{K}_{BA} + \tilde{K}_{BC} + \tilde{K}_{BD} + \tilde{K}_{BE})P_B \quad (36)$$

$$\frac{dP_C}{dt} = \tilde{K}_{AC}P_A + \tilde{K}_{BC}P_B + \tilde{K}_{DC}P_D + \tilde{K}_{EC}P_E - (\tilde{K}_{CA} + \tilde{K}_{CB} + \tilde{K}_{CD} + \tilde{K}_{CE})P_C \quad (37)$$

$$\frac{dP_D}{dt} = \tilde{K}_{AD}P_A + \tilde{K}_{BD}P_B + \tilde{K}_{CD}P_C + \tilde{K}_{ED}P_E - (\tilde{K}_{DA} + \tilde{K}_{DB} + \tilde{K}_{DC} + \tilde{K}_{DE})P_D \quad (38)$$

$$\frac{dP_E}{dt} = \tilde{K}_{AE}P_A + \tilde{K}_{BE}P_B + \tilde{K}_{CE}P_C + \tilde{K}_{DE}P_D - (\tilde{K}_{EA} + \tilde{K}_{EB} + \tilde{K}_{EC} + \tilde{K}_{ED})P_E \quad (39)$$

The probabilities of occupying metabasins α and β are given by eqs 40 and 41, respectively.

$$f_\alpha = P_A + P_B \quad (40)$$

$$f_\beta = P_C + P_D + P_E \quad (41)$$

The rates of change of f_α and f_β are given by eqs 42 and 43, respectively.

$$\frac{df_\alpha}{dt} = (\tilde{K}_{CA} + \tilde{K}_{CB})P_C + (\tilde{K}_{DA} + \tilde{K}_{DB})P_D + (\tilde{K}_{EA} + \tilde{K}_{EB})P_E - (\tilde{K}_{AC} + \tilde{K}_{AD} + \tilde{K}_{AE})P_A - (\tilde{K}_{BC} + \tilde{K}_{BD} + \tilde{K}_{BE})P_B \quad (42)$$

$$\frac{df_\beta}{dt} = (\tilde{K}_{AC} + \tilde{K}_{AD} + \tilde{K}_{AE})P_A + (\tilde{K}_{BC} + \tilde{K}_{BD} + \tilde{K}_{BE})P_B - (\tilde{K}_{CA} + \tilde{K}_{CB})P_C - (\tilde{K}_{DA} + \tilde{K}_{DB})P_D - (\tilde{K}_{EA} + \tilde{K}_{EB})P_E \quad (43)$$

From eq 26, the transition rate $\tilde{K}_{CA}$ is given by eq 44;

$$\tilde{K}_{CA} = g_A K_{i\in C, j\in A} \quad (44)$$

where $i \in$ C is any of the g_C degenerate microstates in C and $j \in$ A is any of the g_A degenerate microstates in A. For simplification of notation, we define K_{CA} in eq 45.

$$K_{CA} \equiv K_{i\in C, j\in A} = \frac{\tilde{K}_{CA}}{g_A} \quad (45)$$

Note that there are only five unique transition rates:

$$K_{CA} = K_{CB} \quad (46)$$

$$K_{DA} = K_{DB} \quad (47)$$

$$K_{EA} = K_{EB} \quad (48)$$

$$K_{AC} = K_{AD} = K_{AE} \quad (49)$$

$$K_{BC} = K_{BD} = K_{BE} \quad (50)$$

Therefore, the set of master equations reduces to eqs 51 and 52.

$$\frac{df_\alpha}{dt} = (g_A + g_B)K_{CA}P_C + (g_A + g_B)K_{DA}P_D + (g_A + g_B)K_{EA}P_E - (g_C + g_D + g_E)K_{AC}P_A - (g_C + g_D + g_E)K_{BC}P_B \quad (51)$$

$$\frac{df_\beta}{dt} = (g_C + g_D + g_E)K_{AC}P_A + (g_C + g_D + g_E)K_{BC}P_B - (g_A + g_B)K_{CA}P_C - (g_A + g_B)K_{DA}P_D - (g_A + g_B)K_{EA}P_E \quad (52)$$

We define n_α as the total number of microstates within metabasin α by eq 53;

$$n_\alpha = \sum_{A\in\alpha} g_A \quad (53)$$

such that

$$\frac{df_\alpha}{dt} = n_\alpha K_{CA}P_C + n_\alpha K_{DA}P_D + n_\alpha K_{EA}P_E - n_\beta K_{AC}P_A - n_\beta K_{BC}P_B \quad (54)$$

$$\frac{df_\beta}{dt} = n_\beta K_{AC}P_A + n_\beta K_{BC}P_B - n_\alpha K_{CA}P_C - n_\alpha K_{DA}P_D - n_\alpha K_{EA}P_E \quad (55)$$

By defining the intermetabasin transition rates as shown in eqs 56 and 57,

$$w_{\alpha\beta} = \frac{n_\beta}{f_\alpha}(K_{AC}P_A + K_{BC}P_B) \quad (56)$$

$$w_{\beta\alpha} = \frac{n_\alpha}{f_\beta}(K_{CA}P_C + K_{DA}P_D + K_{EA}P_E) \quad (57)$$

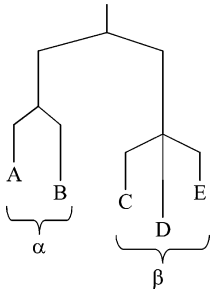

Figure 2. System with two metabasins, α and β.

the set of master equations governing the intermetabasin dynamics can be written in the familiar form shown in eqs 58 and 59.

$$\frac{df_\alpha}{dt} = w_{\beta\alpha}f_\beta - w_{\alpha\beta}f_\alpha \quad (58)$$

$$\frac{df_\beta}{dt} = w_{\alpha\beta}f_\alpha - w_{\beta\alpha}f_\beta \quad (59)$$

In general, the system of master equations in the metabasin approach can be expressed as eq 60;

$$\frac{df_\alpha}{dt} = \sum_{\beta\neq\alpha} (w_{\beta\alpha}f_\beta - w_{\alpha\beta}f_\alpha) \quad (60)$$

where $w_{\alpha\beta}$ is the transition rate from metabasin α to metabasin β, which can computed by eq 61.

$$w_{\alpha\beta} = \frac{n_\beta}{f_\alpha}\sum_{A\in\alpha} K_{A,B\in\beta}P_A \quad (61)$$

Because the metabasins are chosen based on the observation time scale, the integration time step for solving eq 60 is governed by the natural time scale of the experiment (i.e., the inverse of the cooling rate).

4. Metabasin Partitioning

This leaves the important question of how to partition the system into metabasins obeying internal ergodicity. The metabasin partitioning depends on both the instantaneous temperature T and on the time derivative dT/dt. We propose the following algorithm to determine the metabasin partitioning. (The description of the algorithm is followed by a detailed example illustrating the various steps.)

(1) Construct an $N \times N$ rate matrix **K**, where N is the number of states in the system. Note that N may refer to either the total number of microstates (Ω) or the total number of nondegenerate states; the algorithm is independent of whether degeneracy is implicitly or explicity included. The diagonal terms of the rate matrix **K** are zero, and the off-diagonal K_{ij} terms give the transition rates from state i to state j:

$$\mathbf{K} = \begin{pmatrix} 0 & K_{12} & K_{13} & \cdots & K_{17} \\ K_{21} & 0 & K_{23} & \cdots & K_{27} \\ K_{31} & K_{32} & 0 & \cdots & K_{3N} \\ \vdots & \vdots & \vdots & \ddots & \vdots \\ K_{N1} & K_{N2} & K_{N3} & \cdots & 0 \end{pmatrix} \quad (62)$$

Although our algorithm for metabasin partitioning is independent of the particular form of K_{ij}, in general, the transition rate will

decrease Arrheniusly with temperature. Assuming transition state theory, K_{ij} has the form shown in eq 63.

$$K_{ij} = \nu_{ij} \exp\left(-\frac{\Delta U_{ij}}{kT}\right) \tag{63}$$

Here, ν_{ij} is the vibrational frequency, ΔU_{ij} is the activation barrier, k is Boltzmann's constant, and T is the absolute temperature. If we account for degeneracy as in Section 2, K_{ij} adopts the form shown in eq 64.

$$K_{ij} = \nu_{ij} g_j \exp\left(-\frac{\Delta U_{ij}}{kT}\right) \tag{64}$$

In practice it may be more convenient to work with $\ln g_j$ rather than g_j directly. In this case, K_{ij} should be expressed as shown in eq 65.

$$K_{ij} = \nu_{ij} \exp\left(-\frac{\Delta U_{ij}}{kT} + \ln g_j\right) \tag{65}$$

(2) The next step is to rank the transition rates (K_{ij}) from lowest to highest for the current temperature T. Whereas the faster transitions may have time to fully equilibrate at the temperature (T), the slower transitions may not.

(3) Let the instantaneous cooling rate be dT/dt. Transitions with $K_{ij} \gg (1/\Delta T)|\mathrm{d}T/\mathrm{d}t|$ will equilibrate on a time scale faster than the cooling rate. In practice, we choose a threshold rate as shown in eq 66.

$$K^{\mathrm{th}} = \left|\frac{dT}{dt}\right| \cdot 10\ \mathrm{K}^{-1} \tag{66}$$

Transition rates satisfying $K_{ij} > K^{\mathrm{th}}$ are assumed to equilibrate fully during the time step dt, whereas transition rates below the threshold are too slow to equilibrate during dt. (See Section 6 for more information on choosing the time step dt.)

(4) Now that the transition rates are divided into two groups (i.e., above and below K^{th}), we can determine the metabasin partitioning. If no values of K_{ij} fall below K^{th}, then the entire system is in equilibrium, and no metabasin partitioning is necessary. The partitioning is accomplished by first dividing the system into two metabasins. Additional metabasins are subsequently formed, if necessary, through further division of one of the existing metabasins. We accomplish the partitioning by considering first the slowest rates below K^{th}. Recall that the first index i in the rate K_{ij} refers to the initial state for a given transition to some other state j. The rates falling below the threshold may involve one or more different initial states i. When performing the partitioning, we consider only one initial state i at a time, starting with the slowest rates. For example, if the set of rates $\{K_{21}, K_{25}, K_{34}, K_{35}\}$ fall below K^{th}, we should consider either the subset $\{K_{21}, K_{25}\} \equiv K_{2\{j\}}$ for $i = 2$ or the subset $\{K_{34}, K_{35}\} \equiv K_{3\{j\}}$ for $i = 3$. For a given value of i, we may denote the subset of rates below K^{th} as $K_{i\{j\}}$, where $\{j\}$ denotes the set of final states j. Hence, $\{j\}$ gives the set of states that should be part of a separate metabasin from the initial state i. All of the remaining states connected by rates above K^{th} should be part of the same metabasin as i. Thus, we can accomplish the metabasin partitioning by crossing out the j^{th} rows and columns of the original **K** matrix (i.e., all transitions involving $\{j\}$). The **K** matrix divides into two matrices, denoting the two separate metabasins. One matrix is composed of all elements of the original **K** matrix that were not crossed out in step 4. The other matrix is composed of all elements that were crossed out twice (i.e., where both the row and the column fall into $\{j\}$). All other elements of the original **K** matrix (i.e., those crossed out only once) are discarded because they no longer contribute to the metabasin partitioning. Note that the diagonal elements are never discarded because these represent the states themselves (and not the transitions between states). This nonintuitive procedure will be illustrated with a simple example immediately below.

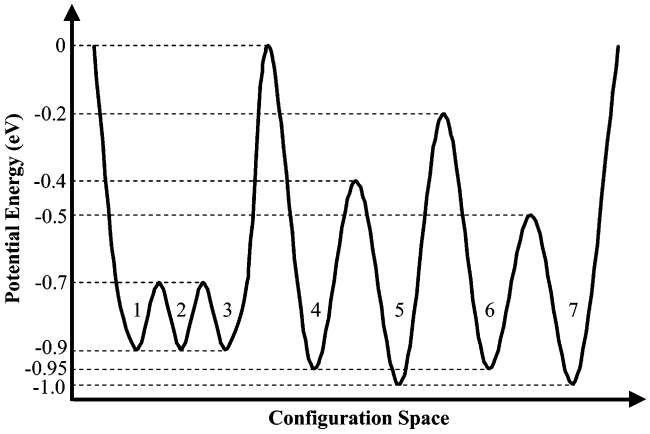

Figure 3. Potential energy landscape with seven basins.

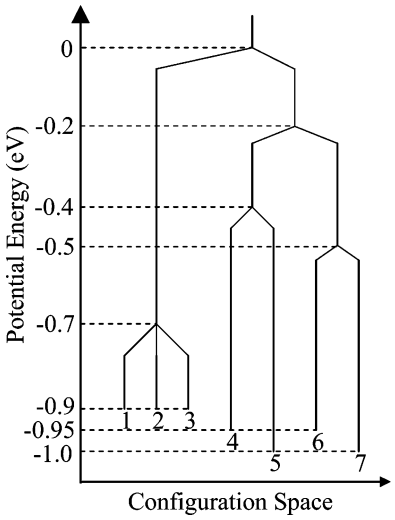

Figure 4. The potential energy landscape of Figure 3, presented in terms of a disconnectivity diagram.

(5) Repeat step 4 recursively for all other values of i where $K_{i\{j\}} < K^{\mathrm{th}}$, proceeding from lowest to highest values of $K_{i\{j\}}$. This may cause the metabasin matrices to subdivide into new metabasins (i.e., new matrices).

(6) Repeat the entire algorithm for each new temperature T.

The above algorithm can be elucidated with the help of a simple example. Figure 3 depicts a simple potential energy landscape with seven basins, arbitrarily labeled from 1 to 7. The landscape can be represented in terms of a disconnectivity graph, as shown in Figure 4. The first step of the algorithm is to construct a 7×7 rate matrix:

$$\mathbf{K} = \begin{pmatrix} 0 & K_{12} & K_{13} & K_{14} & K_{15} & K_{16} & K_{17} \\ K_{21} & 0 & K_{23} & K_{24} & K_{25} & K_{26} & K_{27} \\ K_{31} & K_{32} & 0 & K_{34} & K_{35} & K_{36} & K_{37} \\ K_{41} & K_{42} & K_{43} & 0 & K_{45} & K_{46} & K_{47} \\ K_{51} & K_{52} & K_{53} & K_{54} & 0 & K_{56} & K_{57} \\ K_{61} & K_{62} & K_{63} & K_{64} & K_{65} & 0 & K_{67} \\ K_{71} & K_{72} & K_{73} & K_{74} & K_{75} & K_{76} & 0 \end{pmatrix} \tag{67}$$

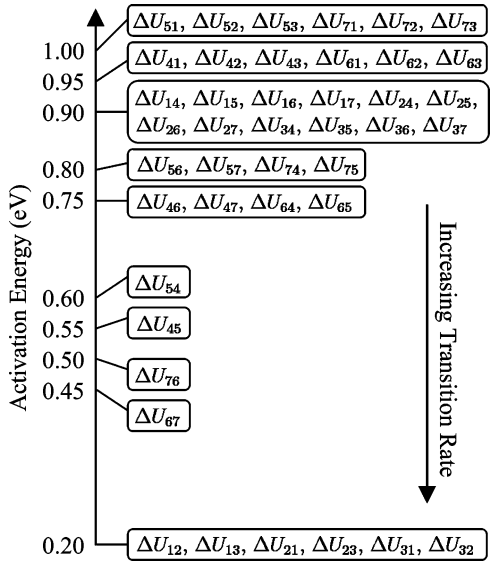

Figure 5. Ranking of the activation energies of the energy landscape of Figure 3. The transition rate increases with decreasing activation energy.

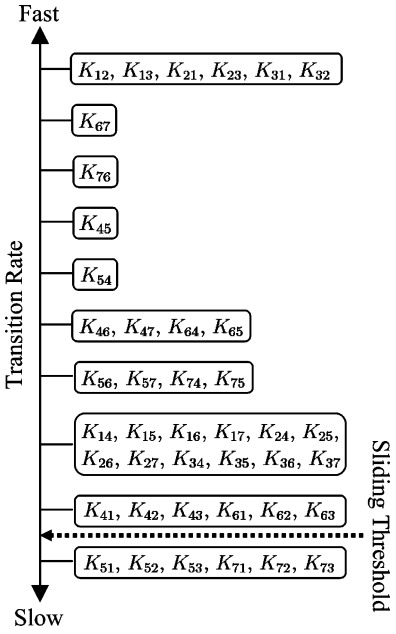

Figure 6. Ranking of the transition rates for the energy landscape in Figure 3. The sliding threshold (K^{th}) depends on both T and dT/dt.

There are $7 \times 6 = 42$ possible transition pathways with 10 unique activation barriers, which are ranked in Figure 5. Assuming the same vibrational frequency along all transition pathways, the K_{ij} rates can be ranked as shown in Figure 6 (step 2 of the algorithm). Let us assume, as in the Mauro−Varshneya[4] approach, that system begins as an equilibrium liquid at the melting temperature. In this case, the threshold rate K^{th} falls below all transition rates K_{ij} such that the system is composed of a single metabasin, indicating a fully ergodic system. As the system is cooled, the first set of K_{ij} values $\{K_{51}, K_{52}, K_{53}, K_{71}, K_{72}, K_{73}\}$ falls below the threshold rate K^{th}, as indicated with the dotted line in Figure 6 (step 3 of the algorithm).

Figure 7 illustrates steps 4 and 5 of the algorithm. From the set of transition values K_{ij} falling below the threshold $\{K_{51}, K_{52}, K_{53}, K_{71}, K_{72}, K_{73}\}$, we pick a subset with a single value of i: $K_{5\{j\}} = \{K_{51}, K_{52}, K_{53}\}$. Thus, the j values to consider in step 4 are $\{j\} = \{1,2,3\}$. Hence, the first, second, and third rows and

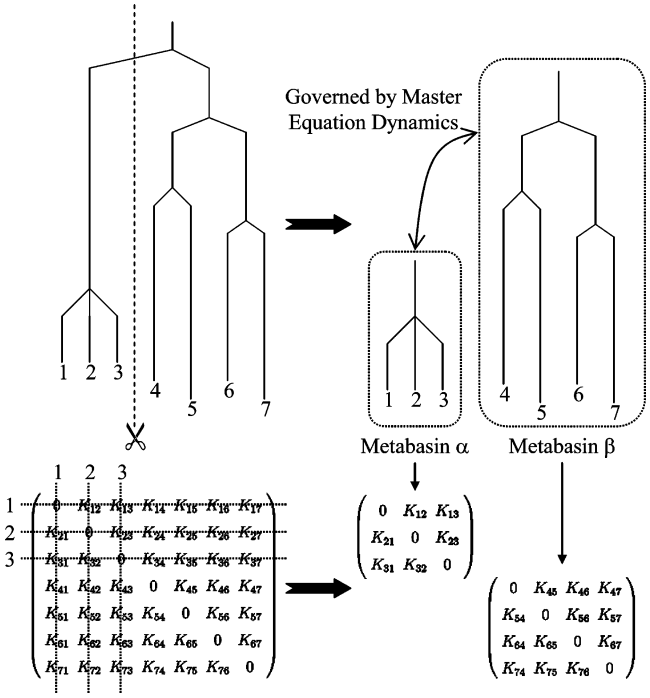

Figure 7. The first partitioning of the energy landscape of Figure 3 into two metabasins, α and β.

columns are crossed out, as shown in Figure 7. In step 5, the original **K** matrix splits into two matrices;

$$\mathbf{K}_{\alpha} = \begin{pmatrix} 0 & K_{12} & K_{13} \\ K_{21} & 0 & K_{23} \\ K_{31} & K_{32} & 0 \end{pmatrix} \tag{68}$$

and

$$\mathbf{K}_{\beta} = \begin{pmatrix} 0 & K_{45} & K_{46} & K_{47} \\ K_{54} & 0 & K_{56} & K_{57} \\ K_{64} & K_{65} & 0 & K_{67} \\ K_{74} & K_{75} & K_{76} & 0 \end{pmatrix} \tag{69}$$

which denote the two metabasins, α and β. The dividing point for the two metabasins is the transition point between basin 5 and basins 1, 2, and 3. All basins falling on the left side of the transition point (1, 2, and 3) are part of metabasin α, and all basins falling on the right side of the transition point (4, 5, 6, and 7) are part of metabasin β. Transitions within both of the metabasins are faster than K^{th}, so intrametabasin ergodicity is maintained. Intermetabasin transitions are computed using a set of two master equations. Step 6 of the algorithm involves repeating steps 4 and 5 for $K_{7\{j\}} = \{K_{71}, K_{72}, K_{73}\}$. However, because $\{j\} = \{1,2,3\}$ is identical to our previous iteration, no new metabasins are formed. (These transition rates were discarded after the first partitioning.) Finally, step 7 of the algorithm states that the algorithm should be repeated at each new temperature.

As the system is cooled, the next set of rate values that drops below the threshold is $\{K_{56}, K_{57}, K_{74}, K_{75}\}$, as shown in Figure 8. (Note that the sets $\{K_{41}, K_{42}, K_{43}, K_{61}, K_{62}, K_{63}\}$ and $\{K_{14}, K_{15}, K_{16}, K_{17}, K_{24}, K_{25}, K_{26}, K_{27}, K_{34}, K_{35}, K_{36}, K_{37}\}$ were discarded in the first metabasin partitioning because these values were singly crossed out in Figure 7 and no longer contribute to the metabasin partitioning.) Of $\{K_{56}, K_{57}, K_{74}, K_{75}\}$, we choose a subset $K_{5\{j\}} = \{K_{56}, K_{57}\}$ giving $\{j\} = \{6, 7\}$. These indices correspond to rows and columns in the $\mathbf{K}_{\beta}$ matrix of eq 69. As

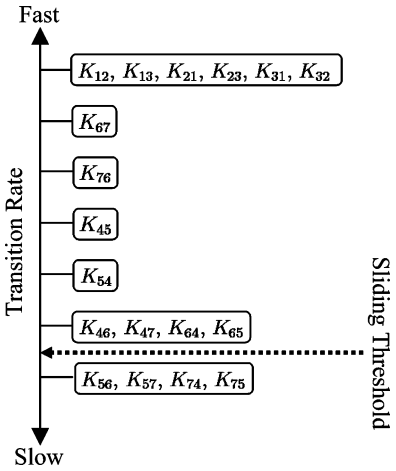

Figure 8. Ranking of the transition rates after the first metabasin partitioning.

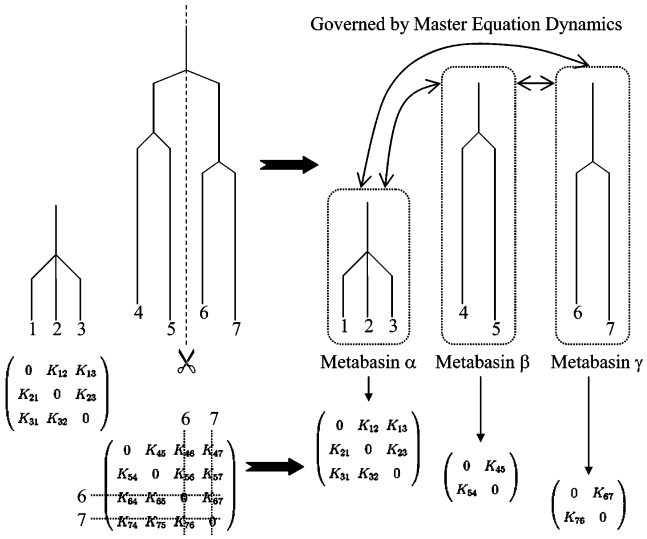

Figure 9. The second partitioning of the example landscape subdivides the second metabasin into two new metabasins. The new metabasins are labeled α, β, and γ.

shown in Figure 9, the second partitioning results in a bifurcation of metabasin β into a new metabasin β

$$\mathbf{K}_\beta = \begin{pmatrix} 0 & K_{45} \\ K_{54} & 0 \end{pmatrix} \tag{70}$$

and a metabasin γ.

$$\mathbf{K}_\gamma = \begin{pmatrix} 0 & K_{67} \\ K_{76} & 0 \end{pmatrix} \tag{71}$$

Note that the same partitioning would result if $K_{7\{j\}} = \{K_{74}, K_{75}\}$ had been used instead of $K_{5\{j\}} = \{K_{56}, K_{57}\}$.

The process continues according to the algorithm above. At a low enough temperature, each metabasin will be composed of only a single basin (1×1 matrix).

5. Approximate Solution for Unbalanced Transition Rates

Thus far, we have considered a clear separation of intra- and intermetabasin relaxation time scales. However, the existence of highly unbalanced intermetabasin transition rates is possible; for example, in Figure 10 the transition rate from α to β is much faster than the rate of reverse transition. In this case, it is possible that $w_{\alpha\beta}$ is greater than the threshold rate K^{th} used for partitioning

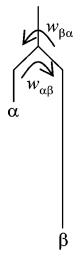

Figure 10. The case of unbalanced transition rates between two metabasins; $w_{\alpha\beta}$ occurs on a time scale much faster than $w_{\beta\alpha}$.

in Section 4, whereas $w_{\beta\alpha}$ falls below the threshold. In this situation, it is not necessary for the α metabasin to have its own master equation, as the solution can be approximated as follows. Considering the direct transitions between metabasins α and β only, we arrive at eqs 72 and 73.

$$\frac{\mathrm{d}f_\alpha}{\mathrm{d}t} = w_{\beta\alpha}f_\beta - w_{\alpha\beta}f_\alpha \tag{72}$$

$$\frac{\mathrm{d}f_\beta}{\mathrm{d}t} = w_{\alpha\beta}f_\alpha - w_{\beta\alpha}f_\beta \tag{73}$$

The solution at the end of the time step dt can be written as eqs 74 and 75;

$$f_\alpha(\mathrm{d}t) = f_\alpha(0) - \mathrm{d}f_{\alpha\beta} \tag{74}$$

$$f_\beta(\mathrm{d}t) = f_\beta(0) + \mathrm{d}f_{\alpha\beta} \tag{75}$$

where $\mathrm{d}f_{\alpha\beta}$ is the transfer of occupation probability from metabasin α to metabasin β. Because $w_{\alpha\beta}$ occurs on a much faster time scale than K^{th}, $\mathrm{d}f_{\alpha\beta}$ can be approximated by application of the detailed balance condition, giving eq 76.

$$\mathrm{d}f_{\alpha\beta} \approx \frac{w_{\alpha\beta}f_\alpha - w_{\beta\alpha}f_\beta}{w_{\alpha\beta} + w_{\beta\alpha}} \tag{76}$$

6. Algorithm for Calculation of the Full System Dynamics

We now provide an algorithm for calculation of the full system dynamics, including intra- and intermetabasin dynamics: (1) Choose a time step dt over which the temperature can be assumed constant. For a constant cooling rate ($\mathrm{d}T/\mathrm{d}t$) we choose $\mathrm{d}t = (0.01\ \mathrm{K})\cdot|\mathrm{d}T/\mathrm{d}t|^{-1}$. (2) At the beginning of the time step, partition the system into metabasins according to the algorithm of Section 4. (3) Redistribute the intrametabasin probabilities according to the equilibrium formulation of eq 31. Use these probabilities and eq 61 to compute the effective intermetabasin transition rates ($w_{\alpha\beta}$). (4) If any of the intermetabasin transition rates ($w_{\alpha\beta}$) fall above the threshold rate K^{th}, then the approximate method of Section 5 can be used to eliminate the α master equation. Repeat step 2. (5) Integrate the reduced set of master equations over the time step dt. We use an integration time step of $\delta t = 0.01 \times \mathrm{d}t$. The intrametabasin probabilities should be redistributed after each δt step using eq 31, and the intermetabasin transition rates should be recomputed using eq 61. (6) Repeat the entire algorithm at each new step in $T(t)$.

7. Validation for a Simple Model Landscape

To validate our algorithm, we compute the dynamics of the system in Figure 3 assuming a vibrational frequency of $\nu_{ij} =$ 0.5 GHz for all transitions and a linear cooling path from 800 to 100 K over a total time of 500 s. Figure 11 shows the resulting

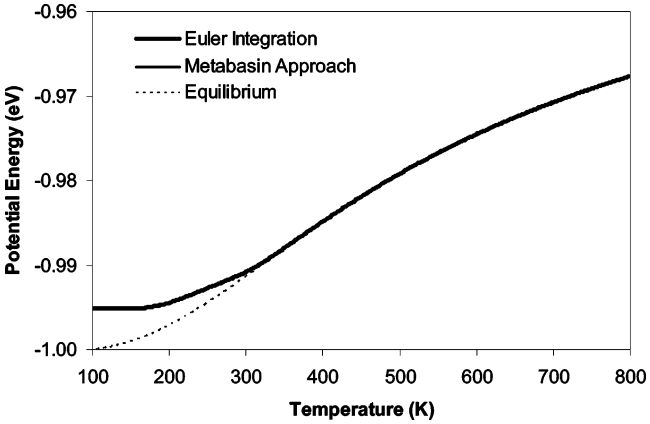

Figure 11. Validation of our metabasin approach versus direct integration of the master equations for the energy landscape in Figure 3.

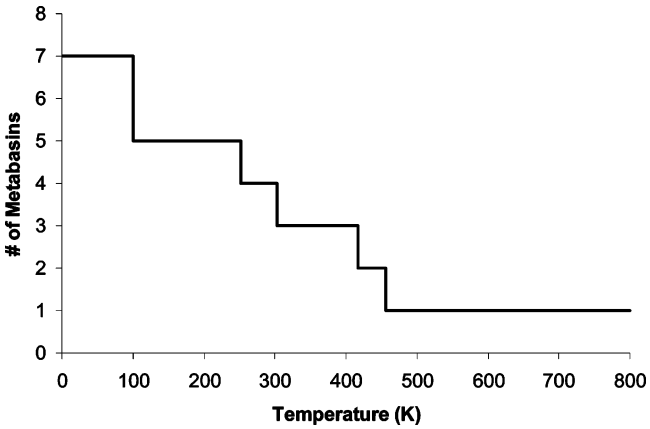

Figure 12. Number of metabasins as a function of temperature, for the calculation of Figure 11.

potential energy of the system as a function of temperature. The average potential energy is computed with the weighted average given by eq 77;

$$\langle U[T(t)]\rangle = \sum_i U_i p_i[T(t)] \tag{77}$$

where U_i denotes the potential energy value associated with the i^{th} microstate. The thick black line shows results computed using the metabasin approach of this manuscript. They are in excellent agreement with results from direct Euler integration of the full set of master equations, shown by the thin gray line. The equilibrium potential energy is shown by the dashed line in this figure. The number of metabasins used in the calculation is shown in Figure 12 as a function of temperature. At high temperatures the system is ergodic, so the entire system consists of just a single metabasin. At very low temperatures every microstate is located in a separate metabasin, so the number of metabasins equals the number of microstates.

8. Application to a Realistic Glass-Forming System

Application of this metabasin technique to realistic glass-forming systems requires enumeration of a sufficient number of inherent structures and transition points in the potential energy or enthalpy landscape.[23] The inherent structures and transition points can be found using a number of standard techniques, such as eigenvector-following.[24−33] However, because the number of inherent structures for an N-particle system scales as $N!\ \exp(\sigma N)$, where σ is a constant,[34] it is impossible to explicitly locate every individual inherent structure. To overcome this difficulty, it is useful to couple the inherent structure calculations with density-of-states calculations to obtain the correct degeneracy values.[35−37] The master equations can then be constructed, incorporating degeneracy as in Section 2.

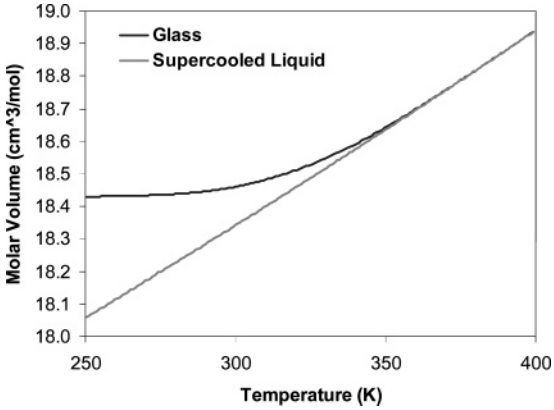

Figure 13. Computed volume−temperature diagram for selenium using a constant cooling rate of 1 K/min. The black curve shows the molar volume of the selenium system as it undergoes a glass transition. This curve is computed using the metabasin approach of this paper. The gray curve shows the molar volume of the supercooled liquid, computed using equilibrium statistical mechanics.

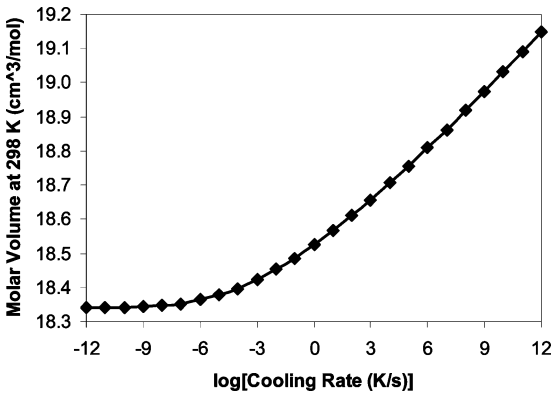

Figure 14. Computed molar volume of selenium after linear cooling from its melting point (490 K) to room temperature (298 K). The cooling rates span 25 orders of magnitude. With the metabasin approach for computing master equation dynamics, each simulation takes approximately 15 min of CPU time.

To demonstrate this technique for a realistic glass-forming system, we consider the case of selenium. By employing the interatomic potentials of Mauro and Varshneya,[38] we consider a system of 64 selenium atoms with periodic boundary conditions. We identify 72 unique inherent structures in the enthalpy landscape, which cover molar volumes from 16.0 to 30.0 cm^3/mol. The degeneracy of the inherent structures is computed using the technique of ref 37 and the total number of inherent structures is estimated to be e^{180}. Transitions between inherent structures are governed by bond angle rearrangements, shown for clusters in ref 39. The master equation dynamics are computed using the metabasin technique above. Figure 13 shows the computed volume−temperature diagram for the selenium system, cooling from 400 to 250 K at a constant rate of 1 K/min. The glass transition occurs around 317 K, which is very close to the experimental value of 318 K.[40] Finally, Figure 14 demonstrates the ability of the metabasin techniqe to handle any cooling rate. (By constrast, traditional techniques such as molecular dynamics and Metropolis Monte Carlo can only achieve extremely fast cooling rates.) This figure shows the final molar volume of the selenium system after cooling from the

melting point (490 K) to room temperature (298 K) with cooling rates varying from 10^{-12} K/s to 10^{12} K/s. Each simulation takes approximately the same CPU time (about 15 min on our workstation). Except for the extremely slowly cooled systems, which equilibrate, the final molar volume of the glass follows an Arrhenius dependence with respect to cooling rate. This result has been previously shown by Moynihan and co-workers[41] with cooling rates that cover 4 orders of magnitude.

The subject of the selenium glass transition is being treated in much greater detail in a forthcoming paper by Mauro and Loucks.

9. Conclusions

We have proposed a technique for solving a system of master equations based on a partitioning of the system into metabasins. The metabasins are chosen such that the relaxation times within a metabasin are short as compared to Δt, the time step over which temperature can be assumed to be constant. In this manner, equilibrium statistical mechanics are assumed within each metabasin, and the intermetabasin dynamics are computed using a reduced set of master equations. The number of metabasins depends on both the temperature of the system and its derivative with respect to time. Our metabasin technique shows excellent agreement with direct Euler integration. Finally, we have demonstrated the technique on a realistic glass-forming system (selenium).

References and Notes

(1) Zwanzig, R. *Nonequilibrium Statistical Mechanics*; Oxford University Press: Oxford, 2001.

(2) Gaveau, B.; Schulman, L. S. *J. Math. Phys.* **1996**, *37*, 3897−3932.

(3) Langer, S.; Sethna, J. P.; Grannan, E. C. *Phys. Rev. B* **1990**, *41*, 2261−2278.

(4) Schnakenberg, J. *Rev. Mod. Phys.* **1976**, *48*, 571−585. .

(5) Van Kampen, N. G. *Stochastic Processes in Physics and Chemistry*; North-Holland: Amsterdam, 1981.

(6) Mauro, J. C.; Varshneya, A. K. *J. Am. Ceram. Soc.* **2006**, *89*, 1091−1094.

(7) Mauro, J. C.; Varshneya, A. K. *Am. Ceram. Soc. Bull.* **2006**, *85*, 25−29.

(8) Gibbs, J. H.; DiMarzio, E. A. *J. Chem. Phys.* **1958**, *28*, 373−383.

(9) Adam, G.; Gibbs, J. H. *J. Chem. Phys.* **1965**, *43*, 139−146.

(10) Götze, W.; Sjögren, L. *J. Phys. C: Solid State Phys.* **1988**, *21*, 3407−3421.

(11) Thirumalai, D.; Mountain, R. D.; Kirkpatrick, T. R. *Phys. Rev. A* **1989**, *39*, 3563−3574.

(12) Van Megen, W.; Underwood, S. M. *J. Phys.: Condens. Matter* **1994**, *6*, A181−A186.

(13) Stein, D. L.; Newman, C. M. *Phys. Rev. E* **1995**, *51*, 5228−5238.

(14) Gupta, P. K.; Mauro, J. C. *J. Chem. Phys.* **2007**, *126*, 224504.

(15) Coluzzi, B.; Crisanti, A.; Marinari, E.; Ritort, F.; Rocco, A. *Eur. Phys. J. B* **2003**, *32*, 495−502.

(16) Mauro, J. C.; Gupta, P. K.; Loucks, R. J. *J. Chem. Phys.* **2007**, *126*, 184511.

(17) Palmer, R. G. *Adv. Phys.* **1982**, *31*, 669−735.

(18) Denny, R. A.; Reichman, D. R.; Bouchaud, J. P. *Phys. Rev. Lett.* **2003**, *90*, 025503.

(19) Doliwa, B.; Heuer, A. *J. Phys.: Condens. Matter* **2003**, *15*, S849−S858.

(20) Doliwa, B.; Heuer, A. *Phys. Rev. E* **2003**, *67*, 031506.

(21) Fabricius, G.; Stariolo, D. A. *Phys. A* **2004**, *331*, 90−98.

(22) Appignanesi, G. A.; Rodríguez Fris, J. A.; Montani, M. A.; Kob, W. *Phys. Rev. Lett.* **2006**, *96*, 057801.

(23) Mauro, J. C.; Loucks, R. J.; Balakrishnan, J.; Varshneya, A. K. *J. Non-Cryst. Solids* **2007**, *353*, 1274−1278.

(24) Wales, D. J. *Energy Landscapes*; Cambridge University Press: Cambridge, 2003.

(25) Schlegel, H. B. *Adv. Chem. Phys.* **1987**, *67*, 249−286.

(26) Cerjan, C. J.; Miller, W. H. *J. Chem. Phys.* **1981**, *75*, 2800−2806.

(27) Simons, J.; Jørgensen, P.; Taylor, H.; Ozment, J. *J. Phys. Chem.* **1983**, *87*, 2745−2753.

(28) O'Neal, D.; Taylor, H.; Simons, J. *J. Phys. Chem.* **1984**, *88*, 1510−1513.

(29) Bell, S.; Crighton, J. S. *J. Chem. Phys.* **1984**, *80*, 2464−2475.

(30) Nichols, J.; Taylor, H.; Schmidt, P.; Simons, J. *J. Chem. Phys.* **1990**, *92*, 340−346.

(31) Banerjee, A.; Adams, N.; Simons, J.; Shepard, R. *J. Phys. Chem.* **1985**, *89*, 52−57.

(32) Mauro, J. C.; Loucks, R. J.; Balakrishnan, J. *J. Phys. Chem. A* **2005**, *109*, 9578−9583.

(33) Mauro, J. C.; Loucks, R. J.; Balakrishnan, J. *J. Phys. Chem. B* **2006**, *110*, 5005−5011.

(34) Stillinger, F. H. *J. Chem. Phys.* **1988**, *88*, 7818−7825.

(35) Wang, F.; Landau, D. P. *Phys. Rev. E* **2001**, *64*, 056101.

(36) Bogdan, T. V.; Wales, D. J.; Calvo, F. *J. Chem. Phys.* **2006**, *124*, 044102.

(37) Mauro, J. C.; Loucks, R. J.; Balakrishnan, J.; Raghavan, S. *J. Chem. Phys.* **2007**, *126*, 194103.

(38) Mauro, J. C.; Varshneya, A. K. *Phys. Rev. B* **2005**, *71*, 214105.

(39) Mauro, J. C.; Loucks, R. J.; Balakrishnan, J.; Varshneya, A. K. *J. Non-Cryst. Solids* **2007**, *353*, 1268−1273.

(40) Senapati, U.; Varshneya, A. K. *J. Non-Cryst. Solids* **1996**, *197*, 210−218.

(41) Moynihan, C. T.; Easteal, A. J.; Wilder, J.; Tucker, J. *J. Phys. Chem.* **1974**, *78*, 2673−2677.